RESEARCH PAPER

# A molecular mechanics approach for analyzing tensile nonlinear deformation behavior of single-walled carbon nanotubes

**Yu Wang · Daining Fang · Ai Kah Soh · Bin Liu**

**Abstract** In this paper, by capturing the atomic information and reflecting the behaviour governed by the nonlinear potential function, an analytical molecular mechanics approach is proposed. A constitutive relation for single-walled carbon nanotubes (SWCNT's) is established to describe the nonlinear stress-strain curve of SWCNT's and to predict both the elastic properties and breaking strain of SWCNT's during tensile deformation. An analysis based on the virtual internal bond (VIB) model proposed by P. Zhang et al. is also presented for comparison. The results indicate that the proposed molecular mechanics approach is indeed an acceptable analytical method for analyzing the mechanical behavior of SWCNT's.

**Keywords** Molecular mechanics approach · Carbon nanotube · Constitutive relation · Young's modulus

## 1 Introduction

Since the discovery [1] of carbon nanotubes (CNT's), there have been an enormous amount of experiments and investigations on the remarkable physical and mechanical properties of CNT's. The Young's modulus of CNT's was found to be about 1 TPa [2–5]. Many theories of mechanics have also been proposed to study the mechanical properties of CNT's. Zhang et al. [6] developed a continuum mechanics approach to model elastic properties of single-walled carbon nanotubes (SWCNT's), and the Young's modulus of SWCNT's was predicted to be 0.705 TPa. Li and Chou [7] presented a structural mechanics approach to model the deformation of CNT's, and calculated the Young's moduli for CNT's with different radii. A similar approach was presented by Chang and Gao [8], and the chirality- and size-dependent elastic properties such as Young's modulus, Poisson's ratio and shear modulus were predicted [9,10]. Moreover, the nonlinear effect of SWCNT's was taken into account [11] recently.

In view of the unrealistic demand of computational power to study materials of practical size, atomistic simulations are deemed unsuitable for the study of large scaled nanometer materials in large time spans. Therefore, various attempts have been made by researchers to introduce atomic characteristics into the mechanical theory. For example, the molecular mechanics originally developed by chemical scientists [12] can be considered one of the successful attempts. According to the definition of Burkert and Allinger [12], the total potential energy, $U$, is constitutive of several individual energy terms corresponding to bond stretching, angle bending, torsion, and van der Waals interactions, respectively:

$$U = \sum U_{\text{stretch}} + \sum U_{\text{bend}} + \sum U_{\text{torsion}} + \sum U_{\text{VDW}}. \tag{1}$$

On the basis of the assumption of small deformation, Li and Chou [7] proposed the following harmonic approximation to describe the energy terms in Eq. (1):

Y. Wang · D. Fang (✉) · B. Liu
Department of Engineering Mechanics, Tsinghua University,
Beijing 100084, China
e-mail: fangdn@mail.tsinghua.edu.cn

A. K. Soh
Department of Mechanical Engineering,
University of Hong Kong, Hong Kong, China

$$U_{\text{stretch}} = \frac{1}{2} k_r (\Delta r)^2,$$

$$U_{\text{bend}} = \frac{1}{2} k_\theta (\Delta \theta)^2, \qquad (2)$$

$$U_{\text{torsion}} = \frac{1}{2} k_\tau (\Delta \phi)^2,$$

where $k_r$, $k_\theta$ and $k_\tau$ are the bond stretching force constant, bond angle bending force constant and torsional resistance, respectively. The symbols, $\Delta r$, $\Delta \theta$ and $\Delta \phi$, represent the bond stretching increment, the bond angle change and the torsion angle change, respectively. Using the classical beam theory, Li and Chou [7] established a direct relationship between the structural mechanics parameters and the molecular mechanics parameters:

$$\frac{EA}{L} = k_r, \quad \frac{EI}{L} = k_\theta, \quad \frac{GJ}{L} = k_\tau. \qquad (3)$$

Thus, Li and Chou [7] modified the molecular mechanics framework and developed a structural mechanics approach for the analysis of mechanical behaviors including elastic moduli, elastic buckling and vibrational behaviors of carbon nanotubes [7,13–18].

By employing molecular mechanics, Chang and Gao [8] studied the elastic properties of an SWCNT subjected to axial loading at small strains. In their analysis, the bond stretching and angle variation terms were taken into account in the total system potential energy, i.e.

$$U_t = \frac{1}{2} \sum_i K_i (\mathrm{d} R_i)^2 + \frac{1}{2} \sum_j C_j (\mathrm{d} \theta_j)^2. \qquad (4)$$

Furthermore, the nonlinear effect was taken into account [11] by constructing the potensial energy function as follows:

$$\begin{aligned}
E &= E_\rho + E_\theta \\
&= \sum_i D_e \left\{ \left[ 1 - \mathrm{e}^{-\beta(\Delta r_i)} \right]^2 - 1 \right\} \\
&\quad + \frac{1}{2} \sum_j k_\theta (\Delta \theta_j)^2 \left[ 1 + k_{\text{sextic}} (\Delta \theta_j)^4 \right].
\end{aligned} \qquad (5)$$

If the molecular mechanics parameters $k_r$, $k_\theta$ and $k_\tau$ in Ref. [7] are assumed to be constants, some important information contained in the nonlinear atomic potential function may be lost. That is, the assumption of small deformation and the negligence of the nonlinear effect of multi-body interatomic potential limit the application range of the molecular mechanics approach. For example, the experimental results [19] and the molecular dynamics (MD) simulations [20,21] show that the axial deformation of carbon nanotubes is nonlinear. To describe the stress–strain curve and predict the breaking strain of carbon nanotubes subjected to tensile loading, some important information contained in the nonlinear atomic potential function must be considered. That is,

the conservative force parameters (for example, $k_r$, $k_\theta$ and $k_\tau$ in Ref. [7]) are no longer constant during deformation.

Compared with the nonlinear potential energy function (in Eq. (5)) applied in Ref. [11], the Tersoff-Brenner (TB) potential [22,23] is applied more widely and more close to the fact. In this study, a molecular mechanics approach based on the TB potential is established and a constitutive relation is developed to predict the nonlinear stress–strain response of different SWCNT's under tensile loading.

## 2 A molecular mechanics approach with consideration of multi-body interatomic potential

By capturing the atomic information and reflecting the behaviour governed by the nonlinear potential function, a new analytical approach is proposed to describe the nonlinear stress–strain curve of SWCNT's and to predict both the elastic properties and breaking strain of SWCNT's during tensile deformation by means of establishing a constitutive relation.

In the study of SWCNT's, TB potential [22,23] is generally adopted to describe the potential between two adjacent carbon atoms $i$ and $j$ as follows:

$$U_{ij} = V_R(r_{ij}) - \bar{b}_{ij}(r_{ij}, \theta_{ijk}) V_A(r_{ij}), \qquad (6)$$

where $r_{ij}$ is the distance between atoms $i$ and $j$; $\theta_{ijk}$ is the angle between bond $i$–$j$ and bond $i$–$k$; $V_R$ and $V_A$ are the repulsive and attractive pair terms; $\bar{b}_{ij}$ represents a multibody coupling between the bond $i$–$j$ and its local environment.

Considering the effect of different atom potentials, the first generation TB potential (TBG1) [22] and the second generation TB potential (TBG2) [23] are applied separately in the proposed molecular mechanics approach to establish the constitutive relations of SWCNT's. Except for employing different versions of the atom potential function, the mathematical manipulation in the molecular mechanics approach is completely same for TBG1 and TBG2. Therefore, only TBG2 is displayed in the following formule manipulation. For comparison, the stress–strain curves obtained from TBG1 and TBG2 will be shown in the same figures. According to the periodic atomic structure of SWCNT's, the deformation within every hexagonal cell in the tube wall is identical under uniform strain fields. The shadow hexagonal cell (Fig. 1) can be taken as a representative cell to study the mechanical behavior of SWCNT's. By summing the atomic potentials of bonds 0–1, 0–2 and 0–3, the total potential of the representative cell can be obtained as follows:

$$\begin{aligned}
&U(r_1, r_2, r_3, \theta_{23}, \theta_{31}, \theta_{12}) \\
&\quad = U_1(r_1, \theta_{31}, \theta_{12}) + U_2(r_2, \theta_{23}, \theta_{12}) + U_3(r_3, \theta_{23}, \theta_{31}),
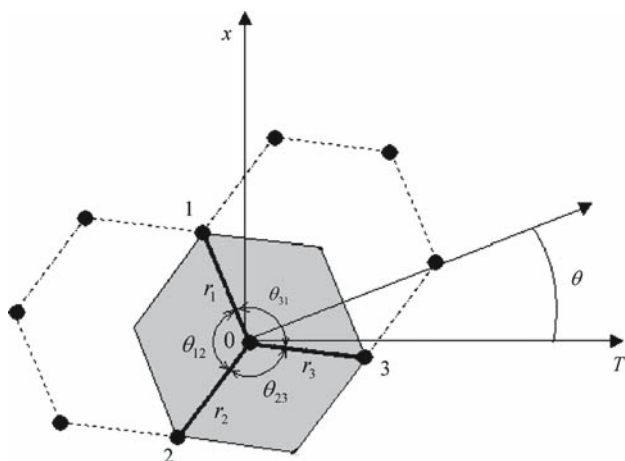\end{aligned} \qquad (7)$$

**Fig. 1** The selected cell within a single-walled carbon nanotube surface

where the variables $r_m$ and $\theta_{mn}$ denote the length of bond 0–$m$ and the angle between bonds 0–$m$ and 0–$n$, respectively. The conservative forces corresponding to the six variables, $r_1, r_2, r_3, \theta_{23}, \theta_{31}, \theta_{12}$, are given by

$$F_{r1} = \frac{\partial U}{\partial r_1}, \quad F_{r2} = \frac{\partial U}{\partial r_2}, \quad F_{r3} = \frac{\partial U}{\partial r_3}, \tag{8a}$$

$$M_{\theta 23} = \frac{\partial U}{\partial \theta_{23}}, \quad M_{\theta 31} = \frac{\partial U}{\partial \theta_{31}}, \quad M_{\theta 12} = \frac{\partial U}{\partial \theta_{12}}. \tag{8b}$$

It is assumed that the adjacent atoms are connected by three line-springs, which have degrees of freedom, $r_1, r_2, r_3$, and internal forces, $F_{r1}, F_{r2}, F_{r3}$. In addition, there are three spiral-springs connecting the adjacent bonds with degrees of freedom, $\theta_{23}, \theta_{31}, \theta_{12}$, and internal moments, $M_{\theta 23}, M_{\theta 31}, M_{\theta 12}$. In accordance with the function of the TB potential, the expressions of the six conservative forces can be deduced as follows:

$$
\begin{aligned}
F_{ri} = {} & [1 + G(\theta_{ij}) + G(\theta_{ki})]^{-\frac{1}{2}}(\beta_1 B_1 \exp(-\beta_1 r_i) \\
& + \beta_2 B_2 \exp(-\beta_2 r_i) + \beta_3 B_3 \exp(-\beta_3 r_i)) \\
& - (\alpha + \frac{\alpha Q}{r_i} + \frac{Q}{r_i^2}) A \exp(-\alpha r_i)
\end{aligned}
$$

$$(i, j, k = 1, 2, 3 \text{ or } 2, 3, 1 \text{ or } 3, 1, 2), \tag{9}$$

$$
\begin{aligned}
M_{\theta ij} = {} & \frac{1}{4}\frac{dG(\theta_{ij})}{d\theta}\{(B_1 \exp(-\beta_1 r_i) + B_2 \exp(-\beta_2 r_i) \\
& + B_3 \exp(-\beta_3 r_i))[1 + G(\theta_{ij}) + G(\theta_{ki})]^{-\frac{3}{2}}) \\
& + (B_1 \exp(-\beta_1 r_j) + B_2 \exp(-\beta_2 r_j) \\
& + B_3 \exp(-\beta_3 r_j))[1 + G(\theta_{jk}) + G(\theta_{ij})]^{-\frac{3}{2}}\}.
\end{aligned}
\tag{10}
$$

It can be shown from Eqs. (9) and (9) that the conservative forces vary nonlinearly during deformation. With the expressions of the conservative forces, one can study the nonlinear

mechanical behavior of nanotubes directly from the equilibrium analysis of conservative forces.

For an SWCNT, van der Waals energy in Eq. (1) can be neglected. The torsional energy may be neglected because it is primarily used to correct the remaining energy terms rather than to represent a physical process in molecular mechanics. Therefore, in the case of an SWCNT subjected to axial loading, only the bond stretching and angle variation terms are significant in the total system potential energy given by Eq. (1). So the total system potential energy of the proposed molecular mechanics approach for analyzing deformation of SWCNT's can be expressed as

$$
\begin{aligned}
U = {} & U_{\text{stretch}} + U_{\text{bend}} \\
= {} & \left( \int_{r_{10}}^{r_1} F_{r1}dr_1 + \int_{r_{20}}^{r_2} F_{r2}dr_2 + \int_{r_{30}}^{r_3} F_{r3}dr_3 \right) \\
& + \left( \int_{\theta_{230}}^{\theta_{23}} M_{\theta 23}d\theta_{23} + \int_{\theta_{310}}^{\theta_{31}} M_{\theta 31}d\theta_{31} + \int_{\theta_{120}}^{\theta_{12}} M_{\theta 12}d\theta_{12} \right).
\end{aligned}
\tag{11}
$$

## 3 Constitutive relations

On the basis of the above proposed molecular mechanics approach, in which the multi-body interatomic potential (TB potential) is employed to consider the nonlinear effect between the consertive force and deformation, the constitutive relations for SWCNT's are established in this section.

### 3.1 Constitutive relation of zigzag SWCNT $(n, 0)$

The conservative forces given by Eqs. (9) and (9) with six variables $r_1, r_2, r_3, \theta_{23}, \theta_{31}, \theta_{12}$ are still valid for SWCNT's. However, the six variables should be expressed in terms of the geometric variables in the cylindrical coordinates of SWCNT's. For the zigzag SWCNT, the geometric variables are $a, h, R$, as shown in Fig. 2(a), and the six variables $r_1, r_2, r_3, \theta_{23}, \theta_{31}, \theta_{12}$ can be expressed by

$$r_1 = a, \quad r_2 = r_3 = \sqrt{2R^2\left(1 - \cos\frac{\pi}{n}\right) + h^2}, \tag{12a}$$

$$
\begin{aligned}
\theta_{31} = {} & \theta_{12} \\
= {} & \arccos\left(-h\Big/\sqrt{2R^2\left(1 - \cos\frac{\pi}{n}\right) + h^2}\right),
\end{aligned}
\tag{12b}
$$

$$\theta_{23} = \arccos\left(\frac{R^2\left(1 - 2\cos\frac{\pi}{n} + \cos\frac{2\pi}{n}\right) + h^2}{2R^2\left(1 - \cos\frac{\pi}{n}\right) + h^2}\right). \tag{12c}$$

Shown in Fig. 3 is the equilibrium diagram of bond 0–2 in the zigzag SWCNT's. Due to the symmetry of both the atomic structure and the applied axial loading, the internal moments
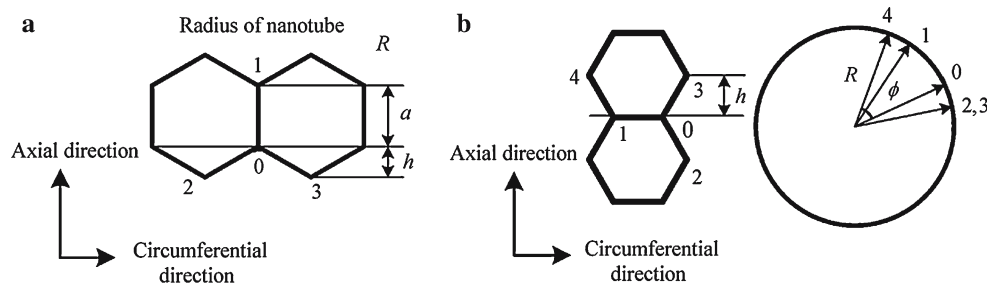
**Fig. 2** Geometric variables under tensile deformation for **a** zigzag SWCNT's; **b** armchair SWCNT's
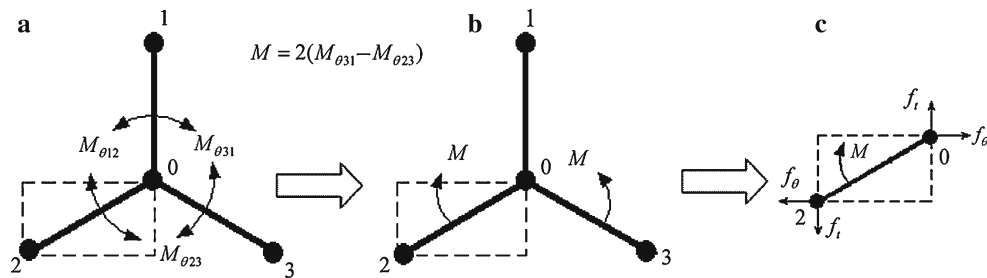


**Fig. 3** Equilibrium analysis of bond 0–2 in zigzag SWCNT's

in the representative cell should satisfy the condition that $M_{\theta23} \neq M_{\theta31} = M_{\theta12}$ (Fig. 3a). If we release the three spiral-springs in the representative cell, there will be three bonds in the cell with no interactions between the adjacent bonds. To replace the action of the released spiral-springs, an equivalent moment of $M = 2(M_{\theta31} - M_{\theta23})$ is applied on bond 0–2 and bond 0–3 (Fig. 3b). Because the forces $F_{r1}$, $F_{r2}$ and $F_{r3}$, are still internal forces of the representative cell, they are not shown in Fig. 3a and Fig. 3b.

As shown in Fig. 3b, a rectangular unit which has a diagonal bond 0–2 is selected to analyze force equilibrium. After bond 0–2 is picked out, bond 0–1 and 0–3 are broken. Therefore, the internal forces $F_{r1}$ and $F_{r3}$ should be added to the edges of the rectanglular unit, their actions can be replaced by $f_t$ and $f_\theta$, which are the stretching forces of the rectanglular unit along the axial and circumferential directions, respectively. Due to the symmetry, the stress state of the rectangular unit which has a diagonal bond 0–3 is completely symmetrical with the above rectangular unit along bond 0–1. In the circumferential direction of SWCNT $(n, 0)$, there are totally $n$ representative cells like that shown in Fig. 3b. Every representative cell shares an axial stretching force $F_{r1} = 2f_t$. Therefore, the axial force of an SWCNT $(n, 0)$ can be directly obtained as

$$P = 2nf_t = nF_{r1}. \tag{13}$$

In addition, the circumferential stress should be zero in the case of tensile loading, i.e. the only circumferential stretching force in the representative cell

$$f_\theta = 0. \tag{14}$$

The moment equilibrium of the rectangular unit which has a diagonal bond 0–2 (Fig. 3c) leads to the following relation:

$$\begin{aligned} M &= 2(M_{\theta31} - M_{\theta23}) \\ &= f_t r_2 \sin\theta_{12} - f_\theta r_2(-\cos\theta_{12}) \\ &= \frac{1}{2} F_{r1} r_2 \sin\theta_{12}, \end{aligned} \tag{15}$$

where $M_{\theta23}$, $M_{\theta31}$ and $F_{r1}$ are

$$\begin{aligned} M_{\theta23} = &\frac{1}{4}\frac{dG(\theta_{23})}{d\theta} \Big\{ (B_1 \exp(-\beta_1 r_2) + B_2 \exp(-\beta_2 r_2) \\ &+ B_3 \exp(-\beta_3 r_2)) [1 + G(\theta_{23}) + G(\theta_{12})]^{-\frac{3}{2}}) \\ &+ (B_1 \exp(-\beta_1 r_3) + B_2 \exp(-\beta_2 r_3) \\ &+ B_3 \exp(-\beta_3 r_3)) [1 + G(\theta_{31}) + G(\theta_{23})]^{-\frac{3}{2}} \Big\}. \end{aligned} \tag{16a}$$

$$\begin{aligned} M_{\theta31} = &\frac{1}{4}\frac{dG(\theta_{31})}{d\theta} \Big\{ (B_1 \exp(-\beta_1 r_3) + B_2 \exp(-\beta_2 r_3) \\ &+ B_3 \exp(-\beta_3 r_3)) [1 + G(\theta_{31}) + G(\theta_{23})]^{-\frac{3}{2}}) \\ &+ (B_1 \exp(-\beta_1 r_1) + B_2 \exp(-\beta_2 r_1) \\ &+ B_3 \exp(-\beta_3 r_1)) [1 + G(\theta_{12}) + G(\theta_{31})]^{-\frac{3}{2}} \Big\}, \end{aligned} \tag{16b}$$

$$\begin{aligned} F_{r1} = &[1 + G(\theta_{12}) + G(\theta_{31})]^{-\frac{1}{2}} (\beta_1 B_1 \exp(-\beta_1 r_1) \\ &+ \beta_2 B_2 \exp(-\beta_2 r_1) + \beta_3 B_3 \exp(-\beta_3 r_1)) \\ &- \left( \alpha + \frac{\alpha Q}{r_1} + \frac{Q}{r_1^2} \right) A \exp(-\alpha r_1). \end{aligned} \tag{16c}$$

Substituting Eq. (12) into Eq. (16), the variables $r_1, r_2, r_3$, $\theta_{23}$, $\theta_{31}$ and $\theta_{12}$ can be replaced by the geometric variables

$R$, $h$ and $a$. If the axial elongation strain is $\varepsilon$ for SWCNT (17, 0), the relations between $\varepsilon$ and the geometric variables $a$, $h$, $R$, are

$$R = R_0(1 - \nu\varepsilon), \tag{17}$$

$$a + h = (a_0 + h_0)(1 + \varepsilon), \tag{18}$$

where $a_0 = 0.145$ nm, $h_0 = 0.0724$ nm, $R_0 = 0.682$ nm are the initial values of $a$, $h$, $R$ for the SWCNT (17, 0). The variables $a$, $h$ and $R$ are such a set of geometric variables that can represent the atom structure of a zigzag SWCNT independently, therefore, the total energy fuction of a zigzag SWCNT can be constructed as $U_{\text{zig}}(a, h, R)$. For a zigzag SWCNT without any loading, its initial atom structure (i.e. $a_0$, $h_0$ and $R_0$) can be obtained according to the extremum principle $\frac{\partial U_{\text{zig}}}{\partial a} = \frac{\partial U_{\text{zig}}}{\partial h} = \frac{\partial U_{\text{zig}}}{\partial R} = 0$.

From Eqs. (13) and (14), the stress state of SWCNT $(n, 0)$ with thickness, $t$, is given by

$$\begin{aligned}
\sigma_t &(R, h, a) \\
&= \frac{nF_{r1}}{2\pi Rt} = \frac{n}{2\pi Rt} \Big\{ (\beta_1 B_1 \exp(-\beta_1 a) \\
&\quad + \beta_2 B_2 \exp(-\beta_2 a) + \beta_3 B_3 \exp(-\beta_3 a)) \\
&\quad \times \left[ 1 + 2G \arccos\left( \frac{-h}{\sqrt{2R^2(1 - \cos(\pi/n)) + h^2}} \right) \right]^{-\frac{1}{2}} \\
&\quad - \left( \alpha + \frac{\alpha Q}{a} + \frac{Q}{a^2} \right) A \exp(-\alpha a) \Big\},
\end{aligned} \tag{19}$$

$$\sigma_\theta = 0,$$

where the angular function, $G(\theta)$, is an empirical function in the expression of TB potential [23] to introduce the multi-body coupling between the bond and its local environment, and the parameters are:

$$\begin{aligned}
&B_1 = 12389\,\text{eV}, \quad B_2 = 18\,\text{eV}, \quad B_3 = 31\,\text{eV}, \\
&\beta_1 = 4.7\,\text{Å}^{-1}, \quad \beta_2 = 1.4\,\text{Å}^{-1}, \quad \beta_3 = 1.4\,\text{Å}^{-1}, \\
&Q = 0.3\,\text{A}, \quad A = 10954\,\text{eV}, \quad \alpha = 4.7\,\text{Å}^{-1}.
\end{aligned}$$

For the SWCNT (17, 0), the geometric variables $a$, $h$ and $R$ are

$$\begin{aligned}
h =\ & A_1(A_3^{-3}(0.22 + 0.645\varepsilon + 2100\varepsilon^2) - 30A_3^{-10}(1 + \varepsilon)^2 \\
& + (10A_2^{-0.06} + 0.04A_2^{-0.02})(1 + \varepsilon)^3)/ \\
& (100A_3^{-10}(A_1(1.9 + 3\varepsilon + \varepsilon^2) - 57 - 160\varepsilon - 150\varepsilon^2) \\
& - (1700A_2^{-0.06} + 6.8A_2^{-0.02})(1 + \varepsilon)^3 \\
& - A_3^{-3}(A_1(0.31 + 0.88\varepsilon + 0.78\varepsilon^2) \\
& + 10.9 + 32\varepsilon + 30\varepsilon^2)), \\
a =\ & (a_0 + h_0)(1 + \varepsilon) - h, \tag{20} \\
R =\ & R_0(1 - \nu\varepsilon),
\end{aligned}$$

where,

$$\begin{aligned}
A_1 &= \sqrt{(19\varepsilon - 100)^2}, \\
A_2 &= \exp(A_1), \\
A_3 &= \exp(1 + \varepsilon).
\end{aligned} \tag{21}$$

Substituting Eqs. (20) and (21) into Eq. (19), the macroscopic stress–strain relation of the zigzag nanotube can, thus, be obtained. The corresponding nonlinear tensile deformation curve will be illustrated in the next section. For any other zigzag SWCNT $(n, 0)$, calculate its initial geometric configuration $a_0$, $h_0$, $R_0$ firstly according to the extremum principle $\frac{\partial U_{\text{zig}}}{\partial a} = \frac{\partial U_{\text{zig}}}{\partial h} = \frac{\partial U_{\text{zig}}}{\partial R} = 0$, and then substitute the calculated $a_0$, $h_0$, $R_0$ into Eq. (19), the stress–strain relation of zigzag SWCNT $(n, 0)$ can be obtained. This is the process of getting the stress–strain relation of zigzag SWCNT $(n, 0)$, it is similar for any armchair SWCNT $(n, n)$.

## 3.2 Constitutive relation of armchair SWCNT $(n, n)$

For an armchair SWCNT, the variables $r_1, r_2, r_3, \theta_{23}, \theta_{31}$ and $\theta_{12}$ in Eqs. (9) and (9) can be expressed in terms of $h, \phi, R$ (Fig. 2(b)), i.e.

$$r_1 = 2R \sin\frac{\phi}{2}, \tag{22a}$$

$$\begin{aligned}
r_2 = r_3 &= \sqrt{2R^2\left(1 - \cos\left(\frac{\pi}{n} - \phi\right)\right) + h^2}, \quad \theta_{31} = \theta_{12} \\
&= \arccos\left( R\left(1 + \cos\frac{\pi}{n} - \cos\left(\frac{\pi}{n} - \phi\right) - \cos\phi\right)\right) \Big/ \\
&\quad \left[ 2\sin\frac{\phi}{2}\sqrt{2R^2\left(1 - \cos\left(\frac{\pi}{n} - \phi\right)\right) + h^2}\, \right],
\end{aligned} \tag{22b}$$

$$\theta_{23} = \arccos\left( \frac{2R^2\left(1 - \cos\left(\frac{\pi}{n} - \phi\right)\right) - h^2}{2R^2\left(1 - \cos\left(\frac{\pi}{n} - \phi\right)\right) + h^2} \right). \tag{22c}$$

Shown in Fig. 4 is the equilibrium diagram of bond 0–2 in SWCNT $(n, n)$. By adopting the above procedure for analyzing a zigzag SWCNT, there are also stretching forces $f_t$ and $f_\theta$ added to the rectangular unit which has a diagonal bond 0–2.

The circumferential stress should be zero in the case of tensile loading. Therefore, the only circumferential stretching force in the representative cell $F_{r1} = 0$, and the only circumferential stretching force in the above rectangular unit, $f_\theta$, is also zero, i.e.

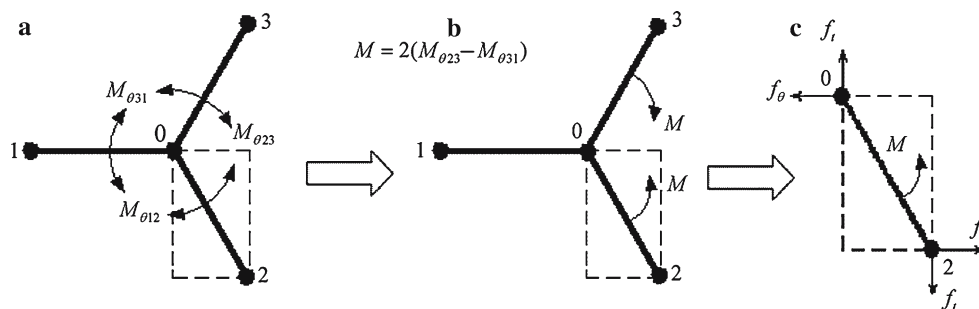$$F_{r1} = f_\theta = 0, \quad (\text{i.e., } \sigma_\theta = 0). \tag{23}$$

**Fig. 4** Equilibrium analysis of bond 0–2 in armchair SWCNT's

Substituting Eq. (22) into Eq. (9) renders

$$
\begin{aligned}
F_{r1} = {}& \left[1 + 2G \arccos\left(R\left(1 + \cos\frac{\pi}{n} - \cos\left(\frac{\pi}{n} - \phi\right) - \cos\phi\right)\right)\right/ \\
& \left.\left(2\sin\frac{\phi}{2}\sqrt{2R^2\left(1 - \cos\left(\frac{\pi}{n} - \phi\right)\right) + h^2}\right)\right]^{-\frac{1}{2}} \\
& \times \left(\beta_1 B_1 \exp\left(-2\beta_1 R \sin\frac{\phi}{2}\right)\right. \\
& + \beta_2 B_2 \exp\left(-2\beta_2 R \sin\frac{\phi}{2}\right) \\
& + \left.\beta_3 B_3 \exp\left(-2\beta_3 R \sin\frac{\phi}{2}\right)\right) \\
& - \left(\alpha + \frac{\alpha Q}{2R\sin\phi/2} + \frac{Q}{(2R\sin\phi/2)^2}\right) \\
& \times A \exp\left(-2\alpha R \sin\frac{\phi}{2}\right),
\end{aligned}
\tag{24}
$$

where $R$, $h$ and $\phi$ are the geometric variables describing the deformation of armchair SWCNT $(n, n)$ under tensile loading. The variables $R$ and $h$ can be expressed directly in terms of the axial elongation strain $\varepsilon$ for SWCNT(10, 10), as follows:

$$
R = R_0(1 - \nu\varepsilon), \tag{25}
$$
$$
h = h_0(1 + \varepsilon), \tag{26}
$$

where $h_0 = 0.1259\,\text{nm}$, $R_0 = 0.694\,\text{nm}$ are the initial values of $h$ and $R$ for SWCNT (10, 10), which can be obtained by the analogous analysis way in zigzag SWCNT's. Note that only two variables, i.e., $\phi$ and $\varepsilon$, are remained in the expression of $F_{r1}$. Substituting Eq. (24) into Eq. (23), we obtain the expression of the variable, $\phi$, in terms of the axial strain, $\varepsilon$,

$$
\phi = 0.23 + 0.043\varepsilon + \frac{C_1}{50} - \frac{1.45 + 1.79\varepsilon - 9.1\varepsilon^2}{100C_1}, \tag{27a}
$$

where

$$
\begin{aligned}
C_1 = {}& ((100\varepsilon^4 - 78\varepsilon^3 + 20\varepsilon^2 - 16\varepsilon + 7.9)^{\frac{1}{2}} \\
& + 9.5\varepsilon^3 - 2.8\varepsilon^2 + 3.1\varepsilon - 2.7)^{\frac{1}{3}}.
\end{aligned}
\tag{27b}
$$

The moment equilibrium equation of the rectangular unit which has a diagonal bond 0–2 (Fig. 4c) is

$$
M + f_\theta r_2 \sin\theta_{12} - f_t r_2(-\cos\theta_{12}) = 0. \tag{28}
$$

In the circumferential direction of SWCNT $(n, n)$, there are totally $2n$ representative cells like that shown in Fig. 4b. Every representative cell shares an axial stretching force $f_t$. Therefore, the axial force of an SWCNT $(n, n)$ is $P = 2nf_t$. Deriving $f_t$ from Eq. (28), the axial force can be expressed by

$$
\begin{aligned}
P = 2nf_t &= \frac{2nM}{r_2(-\cos\theta_{12})} \cong \frac{2nM}{R(\pi/n - \phi)} \\
&= \frac{4n(M_{\theta 23} - M_{\theta 31})}{R(\pi/n - \phi)}.
\end{aligned}
\tag{29}
$$

From Eq. (29) and the zero-stress condition in the circumferential direction (i.e., Eq. (23)), the stress state of SWCNT $(n, n)$ with thickness, $t$, is determined as follows:

$$
\begin{aligned}
&\sigma_t(r_1, r_2, r_3, \theta_{23}, \theta_{31}, \theta_{12}; R, h, \phi) \\
&= \frac{2nf_t}{2\pi Rt} = \frac{nM}{\pi Rr_2t(-\cos\theta_{12})} \cong \frac{nM}{\pi R^2 t(\pi/n - \phi)} \\
&= \frac{2n(M_{\theta 23} - M_{\theta 31})}{\pi R^2 t(\pi/n - \phi)},
\end{aligned}
\tag{30a}
$$
$$
\sigma_\theta = 0,
$$

where $M_{\theta 23}$ and $M_{\theta 31}$ are given by

$$
\begin{aligned}
M_{\theta 23} = {}& \frac{1}{4}\frac{\mathrm{d}G(\theta_{23})}{\mathrm{d}\theta}\{(B_1\exp(-\beta_1 r_2) + B_2\exp(-\beta_2 r_2) \\
& + B_3\exp(-\beta_3 r_2))[1 + G(\theta_{23}) + G(\theta_{12})]^{-\frac{3}{2}} \\
& + (B_1\exp(-\beta_1 r_3) + B_2\exp(-\beta_2 r_3) \\
& + B_3\exp(-\beta_3 r_3))[1 + G(\theta_{31}) + G(\theta_{23})]^{-\frac{3}{2}}\}. \\
\end{aligned}
\tag{30b}
$$
$$
\begin{aligned}
M_{\theta 31} = {}& \frac{1}{4}\frac{\mathrm{d}G(\theta_{31})}{\mathrm{d}\theta}\{(B_1\exp(-\beta_1 r_3) + B_2\exp(-\beta_2 r_3) \\
& + B_3\exp(-\beta_3 r_3))[1 + G(\theta_{31}) + G(\theta_{23})]^{-\frac{3}{2}} \\
& + (B_1\exp(-\beta_1 r_1) + B_2\exp(-\beta_2 r_1) \\
& + B_3\exp(-\beta_3 r_1))[1 + G(\theta_{12}) + G(\theta_{31})]^{-\frac{3}{2}}\}.
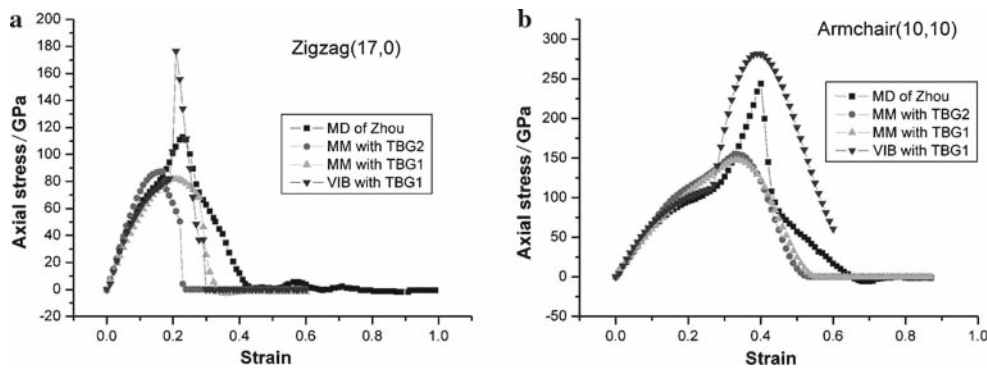\end{aligned}
\tag{30c}
$$

**Fig. 5** Nonlinear tensile stress–strain curves obtained by the molecular mechanics (MM) approach with the first generation TB potential (TBG1) and the second generation TB potential (TBG2), comparing with the virtual internal bond (VIB) calculation and molecular dynamics (MD) simulations for SWCNT's. **a** Zigzag SWCNT (17, 0), **b** Armchair SWCNT (10, 10)

**Fig. 6** The elastic stage of the nonlinear tensile stress–strain curves in Fig. 5 for SWCNT's. **a** Zigzag SWCNT (17, 0), **b** Armchair SWCNT (10, 10)
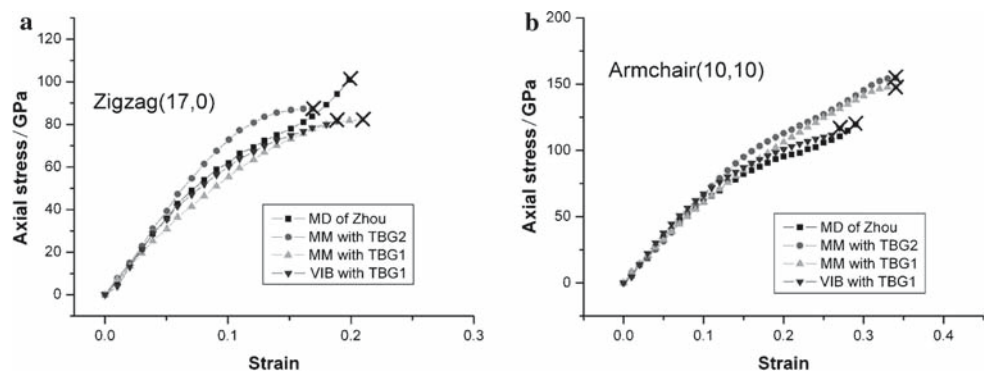


In Eqs. (30b), (30c), the angular function, $G(\theta)$, is an empirical function in the expression of TB potential [23] to introduce the multi-body coupling between the bond and its local environment, and the parameters are:

$$B_1 = 12389 \, \text{eV}, \quad B_2 = 18 \, \text{eV}, \quad B_3 = 31 \, \text{eV},$$
$$\beta_1 = 4.7 \text{Å}^{-1}, \quad \beta_2 = 1.4 \text{Å}^{-1}, \quad \beta_3 = 1.4 \text{Å}^{-1},$$
$$Q = 0.3 \, \text{Å}, \quad A = 10954 \, \text{eV}, \quad \alpha = 4.7 \text{Å}^{-1}.$$

Substituting Eq. (22) and Eqs. (25)–(27) into Eq. (30), a nonlinear stress–strain relation of the armchair nanotube is, thus, obtained. The macroscopic tensile stress–strain curve for the case where $n$ is equal to 10, i.e., armchair nanotube (10, 10), will be shown in the next section.

## 4 Prediction of nonlinear tensile stress–strain curve of SWCNT's

Zhou and Shi [20] performed MD simulations to investigate the stress–strain response of the SWCNT (17, 0) and (10, 10) under tensile loading. The nonlinear tensile stress–strain curves obtained by the proposed molecular mechanics approach are shown in Fig. 5(a) SWCNT (17, 0); (b) SWCNT (10, 10). Considering the effect of different atom potentials,

both of the first generation TB potential (TBG1) and the second generation TB potential (TBG2) are used in the calculations. For the purpose of comparison, an analysis based on the so-called VIB (virtual internal bond) model [6,24], which equates the strain energy at the continuum level to the energy stored in atomic bonds by means of the Cauchy–Born rule, was also carried out in this investigation.

The Young's modulus predicted by using the proposed molecular mechanics approach is about 0.665 TPa for the SWCNT (17, 0), which is close to 0.705 TPa obtained from the VIB approach of Zhang et al. [6]. The tension of an SW-CNT generally undergos three stages: (1) elastic stage (no atom bond breaks); (2) breaking stage (there is an atom bond that starts to break, till the total tube breaks completely); (3) instability stage (the tube loses load-bearing ability). Shown in Fig. 6 is the elastic stage of the nonlinear tensile stress–strain curves in Fig. 5 for SWCNT's: (a) zigzag SWCNT (17, 0), (b) armchair SWCNT (10, 10). Shown in Fig. 7 is the atom structure in the elastic stage of tensile deformation: (a) zigzag SWCNT (17, 0) and (b) armchair SWCNT (10, 10). The first breaking of an atom bond is the transitional point from the elastic stage to the breaking stage. This transitional point appears almost at the same breaking strain for three methods (the molecular mechanics approach, the VIB approach and MD simulations), i.e. it is equal to about
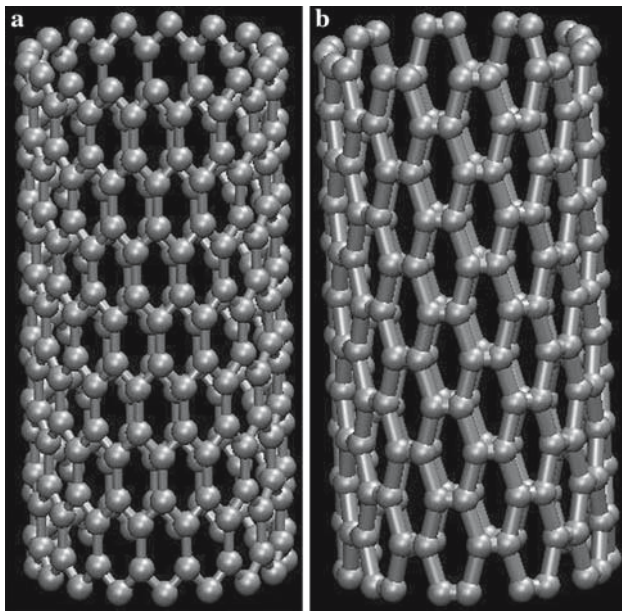
**Fig. 7** The atom structure in the elastic stage of tensile deformation. **a** Zigzag SWCNT (17, 0), **b** Armchair SWCNT (10, 10)

SWCNT's and to predict both the elastic properties and the breaking strain of SWCNT's during tensile deformation. The results presented in Figs. 5 and 6 indicate that the proposed molecular mechanics approach is accurate in embodying the nonlinear characteristics of atomic potential functions, and the predicted stress–strain curves are in a good agreement with those obtained by using molecular dynamics simulations at elastic stage. Both the predicted Young's modulus and the breaking strain of SWCNT's are identical to the analytical results obtained by the VIB approach of Zhang et al. [6] and the MD-simulation results of Zhou and Shi [20]. In addition, every stress-strain curve was calculated in less than 1 minute in terms of the proposed molecular mechanics approach, which reveals that the proposed molecular mechanics approach is also an efficient approach for analyzing the mechanical behavior of SWCNT's. Further work will be performed to extend the proposed molecular mechanics approach to multi-walled carbon nanotubes (MWCNT's).

0.2 ($\varepsilon_b = 0.2$) for SWCNT (17,0) and 0.3 ($\varepsilon_b = 0.3$) for SWCNT (10,10). In the elastic stage, the bonds in the axial direction (i.e. bond 0–1 in Fig. 3) of SWCNT (17,0) become longer and longer (see Fig. 7a) with the increase of loading, and these bonds break firstly at $\varepsilon_b = 0.2$. However, for SWCNT (10,10), the bonds forming an acute angle with the axial direction (i.e. bond 0–2 and bond 0–3 in Fig. 4) become longer and longer (see Fig. 7(b)) during the tensile deformation, and these bonds break firstly at $\varepsilon_b = 0.3$. In the breaking stage, the proposed approach in this study can not describe the complex tensile failure process of the SWCNT, such as "stone-walse" defects or the glide band in SWCNT's, which leads to dishonest predictions of the stress value in this stage. However, in the elastic stage, the stress–strain curves for three approaches are almost completely consistent with each other, while the tensile rigidity of nanotubes for TBG2 appears a little bit higher than that for TBG1.

## 5 Conclusions

Some important information contained in the nonlinear atomic potential function must be considered to describe the nonlinear stress–strain curve and predict the breaking strain of carbon nanotubes subjected to tensile loading. This is because the conservative force parameters are no longer constant during deformation. By capturing the atomic information and reflecting the behaviour governed by the nonlinear potential function, a new molecular mechanics approach is developed to describe the stress–strain curve of

## References

1. Iijima, S.: Helical microtubes of graphitic carbon. Nature **354**, 56–58 (1991)
2. Lu, J.P.: Elastic properties of carbon nanotubes and nanoropes. Phys. Rev. Lett. **79**(7), 1297–1300 (1997)
3. Yakobson, B.I., Brabec, C.J., Bernholc, J.: Nanomechanics of carbon tubes: instability beyond linear response. Phys. Rev. Lett. **76**, 2511–2514 (1996)
4. Yao, N., Vincenzo, L.: Young's modulus of single–walled carbon nanotubes. J. Appl. Phys. **84**(4), 1939–1943 (1998)
5. Treacy, M.M., Ebbesen, T.W., Gibson, J.M.: Exceptionally high Young's modulus observed for individual carbon nanotubes. Nature **381**, 678 (1996)
6. Zhang, P., Huang, Y., Geubelle, P.H., Klein, P.A., Hwang, K.C.: The elastic modulus of single-wall carbon nanotubes: a continuum analysis incorporating interatomic potentials. Int. J. Solids Struct. **39**, 3893–3906 (2002)
7. Li, C.Y., Chou, T.W.: A structural mechanics approach for the analysis of carbon nanotubes. Int. J. Solids Struct. **40**, 2487–2499 (2003)
8. Chang, T.C., Gao, H.J.: Size-dependent elastic properties of a single–walled carbon nanotube via a molecular mechanics model. J. Mechanics Phys. Solids **51**, 1059–1074 (2003)
9. Chang, T., Geng, J., Guo, X.: Chirality- and size-dependent elastic properties of single-walled carbon nanotubes. Appl. Phys. Lett. **87**, 251929 (2005)
10. Chang, T., Geng, J., Guo, X.: Prediction of chirality- and size-dependent elastic properties of single-walled carbon nanotubes via a molecular mechanics model. Proc. R. Soc. A **462**, 2523–2540 (2006)
11. Geng, J., Chang, T.: Nonlinear stick-spiral model for predicting mechanical behavior of single-walled carbon nanotubes. Phys. Rev. B Condens. Matter and Mater. Phys. **74**(24), 245428 (2006)
12. Burkert, U., Allinger, N.L.: Molecular Mechanics. ACS Monograph 177. American Chemical Society, Washington, DC (1982)
13. Li, C.Y., Chou, T.W.: Elastic moduli of multi-walled carbon nanotubes and the effect of van der Waals forces. Compos. Sci. Technol. **63**, 1517–1524 (2003)

14. Li, C.Y., Chou, T.W.: Single-walled carbon nanotubes as ultrahigh frequency nanomechanical resonators. Phys. Rev. B **68**, 073405 (2003)
15. Li, C.Y., Chou, T.W.: Elastic properties of single–walled carbon nanotubes in transverse directions. Physical Review B **69**, 073401 (2004)
16. Li, C.Y., Chou, T.W.: Modeling of elastic buckling of carbon nanotubes by molecular structural mechanics approach. Mechan. Mater. **36**, 1047–1055 (2004)
17. Li, C.Y., Chou, T.W.: Mass detection using carbon nanotube-based nanomechanical resonators. Appl. Phys. Lett. **84**(25), 5246–5248 (2004)
18. Li, C.Y., Chou, T.W.: Vibrational behaviors of multiwalled-carbon-nanotube-based nanomechanical resonators. Appl. Phys. Lett. **84**(1), 121–123 (2004)
19. Pan, Z.W., Xie, S.S., Lu, L., Chang, B.H., Sun, L.F., Zhou, W.Y., Wang, G.: Tensile tests of ropes of very long aligned multiwall carbon nanotubes. Appl. Phys. Lett. **74**(21), 3152–3154 (1999)
20. Zhou, L.G., Shi, S.Q.: Molecular dynamic simulations on tensile mechanicalproperties of single-walled carbon nanotubes with andwithout hydrogen storage. Comput. Materi. Sci. **23**, 166–174 (2002)
21. Yakobson, B.I., Campbell, M.P., Brabed, C.J., Bernholc, J.: High strain rate fracture and C-chain unraveling in carbon nanotubes. Comput. Materi. Sci. **8**, 341–348 (1997)
22. Brenner, D.W.: Empirical potential for hydrocarbons for use in simulating the chemical vapor deposition of diamond films. Phys. Rev. B **42**, 9458–9471 (1990)
23. Brenner, D.W., Shenderova, O.A., Harrison, J.A., Stuart, S.J., Ni, B., Sinnott, S.B.: A second-generation reactive empirical bond order (REBO) potential energy expression for hydrocarbons. J. Phys. Condens. Matter. **14**, 783–802 (2002)
24. Klein, P.A.: A virtual internal bond approach to modeling crack nucleation and growth. Ph.D. dissertation, Stanford University, Palo Alto, CA 94305 (1999)